Separation Science and Technology
Publication details, including instructions for authors and subscription information:
http://www.informaworld.com/smpp/title~content=t713708471

Experimental Study and Mass Transport Modeling of Ethanol Separation from Aqueous Solutions by Pervaporation

Ahmadreza Raisi[ab]; Abdolreza Aroujalian[ab]; Tahereh Kaghazchi[a]
[a] Department of Chemical Engineering, Amirkabir University of Technology (Tehran Polytechnic), Tehran, Iran [b] Food Process Engineering and Biotechnology Research Center, Amirkabir University of Technology (Tehran Polytechnic), Tehran, Iran

To cite this Article Raisi, Ahmadreza , Aroujalian, Abdolreza and Kaghazchi, Tahereh(2009) 'Experimental Study and Mass Transport Modeling of Ethanol Separation from Aqueous Solutions by Pervaporation', Separation Science and Technology, 44: 15, 3538 — 3570
To link to this Article: DOI: 10.1080/01496390903182446
URL: http://dx.doi.org/10.1080/01496390903182446

Separation Science and Technology, 44: 3538–3570, 2009

ISSN: 0149-6395 print/1520-5754 online
DOI: 10.1080/01496390903182446

Taylor & Francis
Taylor & Francis Group

Experimental Study and Mass Transport Modeling of Ethanol Separation from Aqueous Solutions by Pervaporation

Ahmadreza Raisi,[1,2] Abdolreza Aroujalian,[1,2] and Tahereh Kaghazchi[1]

[1]Department of Chemical Engineering, Amirkabir University of Technology (Tehran Polytechnic), Tehran, Iran
[2]Food Process Engineering and Biotechnology Research Center, Amirkabir University of Technology (Tehran Polytechnic), Tehran, Iran

Abstract: Polydimethylsiloxane pervaporation membrane was employed to remove ethanol from aqueous solutions. The influences of feed flow rate, temperature, permeate-side pressure, and ethanol concentration on the membrane performance were investigated. The feed flow rate was shown to have no significant effect on either flux or ethanol selectivity whereas the feed concentration, temperature, and permeate-side pressure had highly significant effects. Sorption and desorption experiments were also performed to provide data for analysis of mass transport based on resistance-in-series model. The analysis of transport resistances revealed that the mass transport of the system was controlled by the transport resistance of components in the membrane active layer.

Keywords: Ethanol/water separation, mass transfer model, pervaporation, resistance-in-series, sorption

Received 29 October 2008; accepted 12 May 2009.

Address correspondence to Abdolreza Aroujalian, Department of Chemical Engineering, Amirkabir University of Technology (Tehran Polytechnic), Hafez Ave., P.O. Box 15875-4413, Tehran, Iran. Tel.: (9821) 64543163; Fax: (9821) 66405847. E-mail: aroujali@aut.ac.ir

INTRODUCTION

Pervaporation technology represents one of the most effective and energy-saving means to separate azeotropic mixtures, close boiling point mixtures, or isomers. For the removal of volatile organic compounds, other separation technologies such as distillation, liquid–liquid extraction, carbon adsorption, and air stripping are not applicable because of feed condition limitations, a large volume of byproducts, or the high cost of post-treatments. However, pervaporation can be applied without these limitations (1). Currently, industrial applications of pervaporation are grouped into three categories, the dehydration of organic solvents using hydrophilic or charged polymeric membranes, the removal of small quantities of volatile organic compounds from water using hydrophobic membranes, and the separation of organic-organic mixtures (2).

The separation of ethanol/water mixtures by pervaporation has been extensively studied (3–11). Many authors reported pervaporation process principals and experimental results using different membranes. For example, Goncalves et al. (3) used silicone rubber and regenerated cellulose film to concentrate ethanol/water solutions and Molina et al. (9) used CMG-OM-010 and 1060-SULZER membranes for feed mixtures contain 13–20%wt. alcohol in water.

Pervaporation is one of the membrane separation processes involving the partial vaporization of a liquid mixture through a dense membrane whose downstream side is usually kept under vacuum. In general, separation by pervaporation can be performed using membranes based on the solution-diffusion mechanism of transport. The steady state mass transport regime depends on several parameters such as the feed-side pressure, the permeate-side pressure, temperature, the properties of the solvent molecule, and the membrane materials. Consequently, the mass transport through a composite polymer membrane is a complex process.

Mass transport mechanism of the pervaporation system can be simply studied by applying resistance-in-series model which allows for the calculation of mass transport resistances in the liquid boundary and in the composite membranes (12,13). The resistance-in-series model, first introduced for membranes in connection with gas separation by Henis and Tripodi (14) has been applied to the pervaporation process by Gudematsch et al. (15). Liu et al. (12) developed a comprehensive resistance-in-series model that included all the steps of the process except the one involving the transport of the vapor from the transmembrane side of a composite membrane to the condensing surface. The resistance offered by this step, however, is generally regarded as small (16). The

liquid boundary layer resistances due to concentration polarization may be insignificant because of low permeation flux. This was confirmed by Jiraratananon et al. (13) that in pervaporation dehydration of ethanol solutions by the composite membranes, transport resistances of the liquid boundary layer were negligible. However, Raghunath and Hwang (17) reported that the hydrodynamic conditions on the feed side or the liquid boundary resistances contributed significantly to the total transport resistances. The primary transport resistance of pervaporation is often assumed to be in the membrane itself (18,19). Pervaporation membrane is usually composite and transport through the active layer of a composite membrane can be described by the widely accepted solution–diffusion model (18). Several works has been shown that the properties of porous supports of composite membranes such as porosity affected pervaporation flux and selectivity (20–22) and porous support resistance may not be neglected.

In order to scale up the experimental results obtained in the laboratory for industrial applications, certain process parameters need to be optimized and reliable mathematical models are necessary to predict the influence of the key parameters. The objectives of this work are:

1. to investigate the effects of various operating parameters such as feed concentration, feed temperature, permeate-side pressure and Reynolds number (feed flow rate) on the permeation flux and ethanol selectivity of a commercial PDMS membrane for separation of ethanol from its aqueous solutions; and
2. to analyze the mass transport resistances and study the transport mechanisms in the composite membrane.

MASS TRANSFER MODEL

Based on the resistance-in-series model, a five-step mechanism is generally assumed to describe the mass transfer of components through a membrane by pervaporation, as shown in Fig. 1. According to this model, the transport of components from the feed solution through the composite membrane occurs by the following steps (12):

1. diffusion through the liquid boundary layer,
2. sorption into the membrane active layer,
3. diffusion of liquid through the membrane active layer,
4. desorption out of the active layer, and
5. transport of vapors through the porous support.

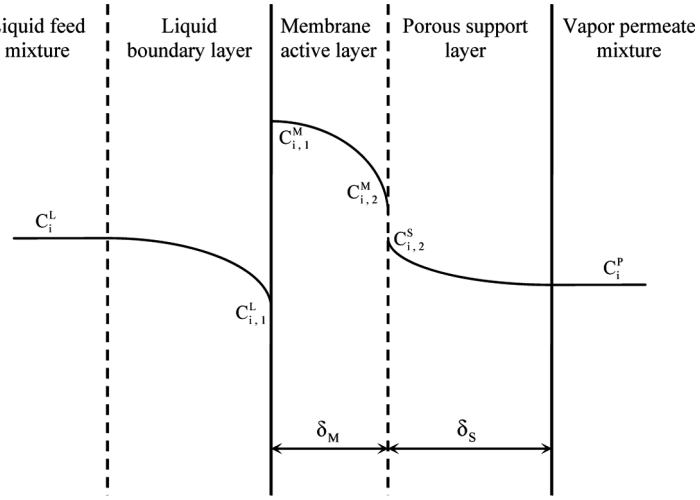

Figure 1. Concentration profile across the pervaporation membrane.

Diffusion Through the Liquid Boundary Layer

At steady state, the sum of convective and diffusive transport in the boundary layer equals the amount of permeated through the membrane. This steady state is expressed for each component by the equation:

$$v_p C_i^L - D_i \frac{dC_i^L}{dz} = v_p C_i^P \tag{1}$$

where v_p is the convective velocity in the boundary layer generated by the permeate flow, which is equal to J/C_L. The mass balance equation for the boundary layer, Eq. (1), can be integrated over the thickness of the boundary layer to give the well-known polarization equation first derived by Brian (23) for reverse osmosis:

$$\frac{C_{i,l}^L - C_i^P}{C_i^L - C_i^P} = \exp(v_p/k_L) \tag{2}$$

The diffusive flux of component *i* through the liquid boundary layer is expressed as:

$$J_i = k_L\left(C_i^L - C_{i,1}^L\right) \tag{3}$$

Two assumptions are implied in the above equation. First, the diffusion coefficient of the component *i* in the boundary layer is independent of

Table 1. Variables for the Sherwood correlation for plate and frame modules

Flow regime	a′	b′	c′	d′
Laminar ($Re < 2300$)	1.615	0.33	0.33	0.33
Turbulent ($Re > 2300$)	0.026	0.80	0.30	–

its concentration, and second the convective flux is negligible. To incorporate the contribution of convective transport the concentration polarization equation, Eq. (2), is substituted into Eq. (3) and rearrange to give:

$$J_i = \frac{v_p}{(\exp(v_p/k_L) - 1)(1 - (1/\beta_i))}\left(C_i^L - C_{i,1}^L\right) \tag{4}$$

The Sherwood correlation has been used to determine the mass transfer coefficient through the boundary layer (24):

$$Sh = a' Re^{b'} Sc^{c'} \left(\frac{d_h}{L}\right)^{d'} \tag{5}$$

The constants a′, b′, c′, and d′ for the Sherwood correlation are given in Table 1.

Sorption into the Membrane Active Layer

There is thermodynamic phase equilibrium between the feed mixture and the polymeric membrane at the liquid boundary/membrane active layer interface. By assuming that the equilibrium establish rapidly, thus no transport resistance is considered for this mass transfer step.

Diffusion Through the Membrane Active Layer

Supposing that transport in the membrane is unidirectional, isothermal and results from a concentration gradient across the membrane. At steady state, the flux of each component can be described as:

$$J_i = \frac{D_i^M}{\delta_M}(C_{i,1}^M - C_{i,2}^M) \tag{6}$$

where D_i^M is the diffusion coefficient of component *i* in the active layer. The diffusion coefficient can be predicted by the free volume theory. This is described in more detail later in this paper.

Desorption out of the Active Layer

For most pervaporation systems, no transport resistance is usually assumed for desorption of liquid molecules at the membrane active layer/support interface since the pressure in the porous support is near the vacuum as in the permeate-side.

Transport of Vapors Through the Porous Support

The support layer is usually microporous with an average pore size $<1\,\mu m$. The mass transport through the porous support should be controlled by either Knudsen diffusion or viscous flow. Any theoretical study of vapor permeation through microporous structures begins with a comparison of the mean free path of the component and the mean pore size of the structure. If the mean free path of the component is much less than the pore size, then the dominant flux mechanism is viscous flow. If the mean free path is much greater than the pore size, then Knudsen diffusion is the dominant mechanism. In this study, the mean free path of ethanol and water in porous support and the mean pore size of the support layer are 10^{-6} and $10^{-9}\,m$, respectively. Thus, the dominant flux mechanism of vapor transport is the Knudsen flow in which the flux equation is (25):

$$J_i = \frac{d_p \varepsilon}{3\delta_S \chi}\left(\frac{8RT_S}{\pi M_i}\right)^{0.5}\left(C_{i,2}^S - C_i^P\right) \tag{7}$$

Although the vapor phase mass transfer coefficient is greater than the mass transfer coefficient in the active layer, the vapor diffusion distance is much longer than the active layer thickness. This resistance could therefore be relatively important, especially when the active layer permeability is high (12).

Combining Eqs (1), (3), and (4) into a single equation gives a relation which is similar to conventional heat and mass transfer equations, which express fluxes as a ratio of the driving force over the total mass transfer resistance, as follows:

$$J_i = \frac{C_i^L - C_i^P}{R_i^T} \tag{8}$$

$$R_i^T = R_i^L + R_i^M + R_i^S \tag{9}$$

where the partial resistance for the boundary layer, the membrane active layer, and the support layer are defined, respectively, as:

$$R_i^L = \frac{(\exp(v_p/k_L) - 1)(1 - (1/\beta_i))}{v_P} \tag{10}$$

$$R_i^M = \frac{\delta_M}{D_i^M \beta_i^M} \tag{11}$$

$$R_i^S = \frac{3\delta_s \chi}{d_p \varepsilon} \left(\frac{\pi M_i}{8RT_s}\right)^{0.5} \tag{12}$$

Modeling of Solutions

In the resistance-in-series model, it is assumed that there is thermodynamic phase equilibrium between the feed mixture and membrane, which indicate that the chemical potential in both phases for component *i* is equal. The volume fraction of component *i* in the membrane is obtained according to the chemical potential equilibrium which can be expressed by the activity equilibrium:

$$a_i^F = a_i^M \tag{13}$$

The activity of each component in the feed mixture and in the membrane is calculated by using UNIFAC (26) and UNIFAC-FV method (27), respectively.

Modeling of Diffusion in Membrane

The free volume theory is widely used in predicting diffusion coefficients of a small molecule through polymers. The concept to describe molecular diffusion by free volume theory was introduced by Cohen and Turnbull (28). Vrentas and Duda (29) extended this concept to describe molecular transport in concentrated polymer solutions. Vrentas et al. (30) have extended this model to predict diffusion coefficients in multicomponent systems from binary free volume data. Based on this model, extensions with thermodynamic factors were proposed in recent years by, e.g. Zielinski and Hanley (31) to describe the multicomponent transport processes. Thermodynamic factors are calculated by means of friction coefficients with different assumptions and rules, e.g. a constant ratio of molecular masses as one possible assumption. In this study, the

Table 2. Free volume parameters for PDMS/ethanol/water system

Parameter	Ethanol (i)	Water (j)	PDMS (p)
$\widehat{V}^*$ (cm^3/g)	0.987	1.072	0.905[a]
K_I/γ ($cm^3/g{\cdot}K$)	3.12×10^{-4}	2.18×10^{-3}	9.32×10^{-4}[b]
K_{II}-T_g (K)	111.80	−152.29	−81.00
ξ_{ip}	0.545	0.232	–
D_o (m^2/s)	11.5×10^{-8}	8.6×10^{-8}	–
E (cal/mol)	188.58	250.01	–

[a]Hong (32).
[b]Zielinski and Duda (31).

fundamental approach of Vrentas et al. (30) is used to calculate the diffusion coefficient of components in a ternary polymer–solvent–solvent system, calculated as follows:

$$D_i = D_{oi}\exp\left(-\frac{E_i}{RT}\right)\cdot\exp\left(-\frac{w_i\widehat{V}_i^* + (\xi_{ip}/\xi_{jp})w_j\widehat{V}_j^* + \xi_{ip}w_p\widehat{V}_p^*}{\widehat{V}^{FH}/\gamma}\right) \quad (14)$$

$$D_j = D_{oj}\exp\left(-\frac{E_j}{RT}\right)\cdot\exp\left(-\frac{(\xi_{jp}/\xi_{ip})w_i\widehat{V}_i^* + w_j\widehat{V}_j^* + \xi_{jp}w_p\widehat{V}_p^*}{\widehat{V}^{FH}/\gamma}\right) \quad (15)$$

$$\begin{aligned}\frac{\widehat{V}^{FH}}{\gamma} &= w_i\frac{K_{I,i}}{\gamma}(K_{II,i} - T_{g,i} + T)\\ &\quad + w_j\frac{K_{I,j}}{\gamma}(K_{II,j} - T_{g,j} + T) + w_p\frac{K_{I,p}}{\gamma}(K_{II,p} - T_{g,p} + T)\end{aligned} \quad (16)$$

The indexes are used as following in this study PDMS (p)-ethanol (i)-water (j). Details about calculation of free volume parameters can be found in Vrentas et al. (30) and Hong (32), the parameters used in this study are presented in Table 2.

MATERIALS AND METHODS

Materials

The PDMS/PVDF/PP composite membrane with a functional layer of polydimethylsiloxane (10 μm thickness) used in the experiments was kindly supplied by GKSS Forschungszentrum (Geesthacht, Germany). The membrane was cut into a 15 × 20 cm piece and held in a flat frame

membrane module. Ethanol (99.8%) was purchased from Merck Co. Ltd. (Darmstadt, Germany) and deionized laboratory water was used for making aqueous mixtures.

Sorption Experiments

To determine the amount of ethanol/water mixture absorbed in the PDMS layer of the composite membrane, swelling measurements of the membranes were performed by a well-known gravimetric procedure. Membrane samples were dried in an oven at 60°C for 5 h to obtain the dried weight and immersed in the liquid mixture in a tightly closed bottle. The composition of the liquid mixture was kept constant at the equilibrium by using a sufficiently large amount of the starting mixture (about 200 ml for 4–5 g membrane). The amount of membrane was calculated to provide at least 0.5 g of the absorbed liquid. The bottles were held into a thermally controlled oven at 30°C. The piece of membrane was then removed from the liquid bath, very quickly blotted with filter paper to remove the superficial liquid, and weighed in a tightly closed bottle (accuracy 0.1 mg). This procedure was then repeated until a constant weight was reached. The thermodynamic equilibrium was usually attained after 3 or 4 days. The liquid sorption value in terms of penetrant volume fraction in the swollen membrane material was then calculated from the polymer mass uptake at equilibrium.

The swelling contribution of each component was then determined after desorption in a glass apparatus composed of a desorption tube and a cold finger trap that can be separated from each other by a valve. The desorbed liquid was recovered under vacuum by cold condensation (liquid nitrogen) and allowed to warm to room temperature under atmospheric pressure. The composition of the desorbed mixture was analyzed by gas chromatography. The above procedures were repeated for different temperatures of 40, 50, and 60°C. The sorption results were reported as the ratio of the liquid weight sorbed per gram of dry membrane and as sorption selectivity. The latter was expressed as:

$$\alpha_{i,j}^{S} = \frac{x_i^M / x_j^M}{x_i^F / x_j^F} \tag{17}$$

Pervaporation Experiments

The pervaporation apparatus has been previously described in Aroujalian et al. (33) and Aroujalian and Raisi (34). The total flux and

ethanol selectivity were calculated using the following equations, respectively:

$$J = \frac{W}{S\tau} \tag{18}$$

$$\alpha_{i,j} = \frac{x_i^P / x_j^P}{x_i^F / x_j^F} \tag{19}$$

In this study, the effect of the feed flow rate (Reynolds number of 500, 1000, 1500, 2000, 2200, and 2500), the feed ethanol concentration (2, 5, 25, 50, 70, and 100%wt.), the feed temperature (30, 40, 50, and 60°C), and the permeate-side pressure (1, 10, 20, and 40 mmHg) on the flux and ethanol selectivity was determined. All experimental conditions were repeated three times and the average values are reported. Steady-state permeation was reached in second hours at all experimental conditions. The time duration of each experiment was 8 hours and a permeate sample was collected every one hour.

Sample Analysis

The collected frozen permeate was melted and weighed. One mL of each sample was diluted ten-fold while the remaining sample was returned to the feed tank to maintain constant initial ethanol concentration. Ethanol concentrations in the diluted permeates were analyzed in triplicate using a Gas Chromatography (Younglin 6000 M Series Gas Chromatography System, Anyang, Korea) equipped with a FID detector and a TRB-Wax capillary column (Teknokroma, Barcelona, Spain) 60 m × 0.32 mm ID × 0.5 μm film thickness. Helium with column head pressure of 10 psi was used as the carrier gas. The injector and the detector temperatures were both 170°C and the oven temperature was 35°C.

Physical Properties

Some physical properties of aqueous ethanol solutions are required for the calculations of mass transport resistance. Viscosities of aqueous ethanol solutions were calculated based on Teja and Rice method (35) and the densities of these solutions were estimated from the equation (36):

$$\rho_m = \sum_i w_i \rho_i \tag{20}$$

Also, the diffusion coefficient of ethanol in water was calculated by the Wilke-Chang equation and the Hsu-Chen method was used to calculate the concentration dependence of the diffusion coefficient (35). The mean free path of water and ethanol vapor in the porous support layer were calculated based on the equation proposed by Kennard (37).

RESULTS AND DISCUSSION

Sorption of Ethanol/Water Mixtures

Sorption experiments were carried out at the temperature range of 30–60°C over the entire composition range using the pure PDMS membrane. Liquid sorption experimental data are presented in Figs. 2 and 3. As shown in Fig. 2a, the total and ethanol sorptions enhanced as ethanol concentration in liquid mixtures increased, but the water sorption curve showed a maximum, which indicates that the strong affinity between water and ethanol molecules could overcome the repellent force of the membrane matrix, and reached a sorption equilibrium. Water sorption was higher than ethanol sorption at low ethanol concentrations in liquid mixtures. Under the same solvent activity, the ethanol will have higher sorption in the PDMS than water does, as shown in Fig. 2a for 0 and 100% feed solutions. Here, at a low ethanol concentration (and also a low activity), the water exhibited higher sorption because of its higher activity. In addition, the plasticization effect exerted by the presence of a small amount of ethanol also enhanced the water sorption, as evidenced in the maximum water sorption in Fig. 2a. The concentration dependence of the sorption curves at a higher temperature had similar trends as the temperature of 30°C.

Variation of sorption selectivity as a function of the feed mixture composition is depicted in Fig. 2b. This figure showed that the sorption selectivity decreased with an increase in the feed ethanol concentration. This may be due to increase in swelling which causes loosening of the polymer matrix, easing the sorption of both the permeants.

All sorptions increased with temperature while the sorption selectivities had no significant changes as shown in Fig. 3. According to the free volume theory (29) an increase of temperature can enhance the thermal motion of the polymer chains, and thus more free volume is generated in the polymer matrix to facilitate the sorption of permeants in the membranes. Therefore, the sorption of both permeants, ethanol and water, enhances as the feed temperature goes to higher levels and consequently, the sorption selectivity that can be related to the ratio of ethanol sorption to water sorption dose not significant changes with temperature.

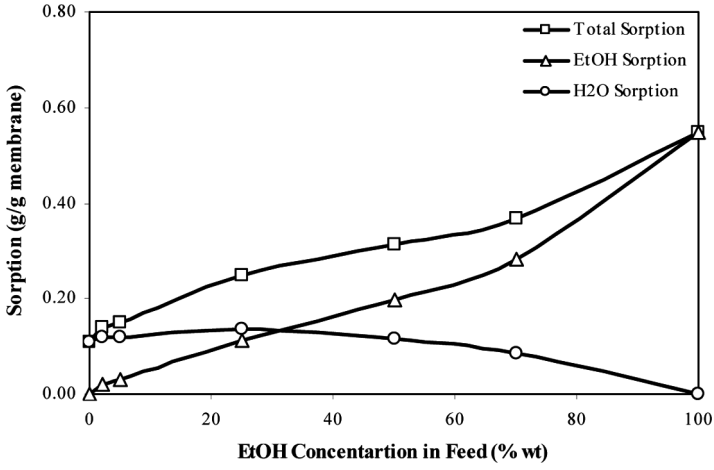

(a)

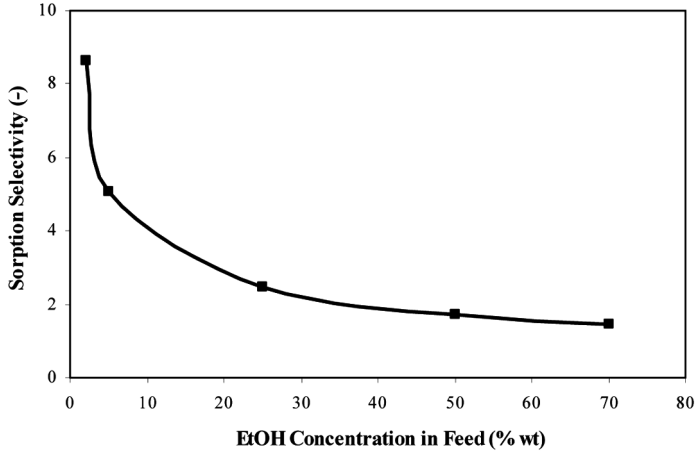

(b)

Figure 2. Effect of ethanol concentration in feed mixture on liquid sorption (a) and sorption selectivity (b) (T = 30°C).

Pervaporation of Ethanol/Water Mixtures

For comparison purpose, the pervaporation performance of the different PDMS membrane reported by other research groups for separating ethanol/water mixtures are listed in Table 3. It can be seen that the ethanol selectivity of the composite PDMS-PVDF-PP membrane is higher than those of most PDMS supported and unsupported membranes reported

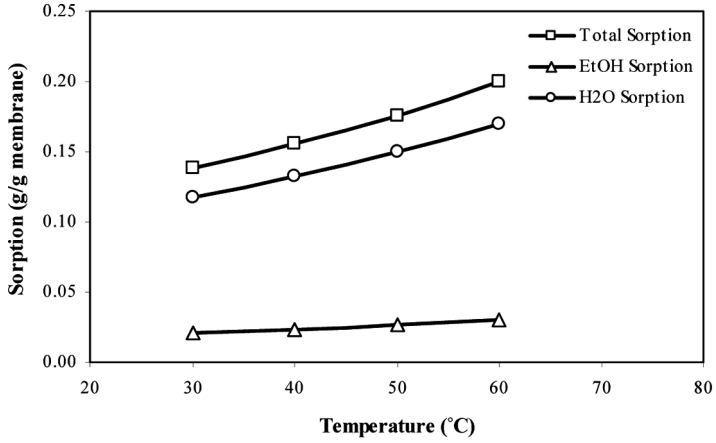

(a)

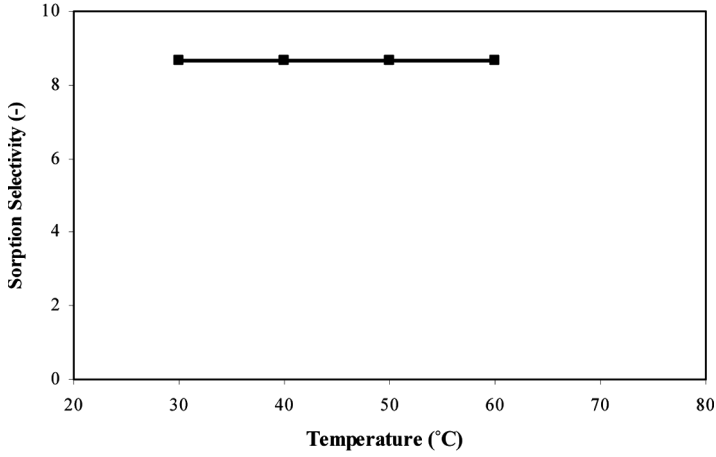

(b)

Figure 3. Effect of temperature on (a) liquid sorption and (b) sorption selectivity ($C_o = 2\%$wt.).

in the literature. In the case of the ethanol separation from 5%wt. ethanol solutions at feed temperature of 60°C under the permeate-side pressure of 1 mmHg, the composite PDMS-PVDF-PP membrane with dense layer thickness of 10 μm in this study has a total flux of $800\,g/m^2 \cdot h$ and a selectivity of 7.8 for ethanol. In the following, the influence of various operating parameters on pervaporative performance of this PDMS composite membrane is explained.

Table 3. Pervaporation performance of different PDMS membranes

Membrane	Membrane thickness (μm)	Ethanol concentration in the feed (%wt.)	Temperature (°C)	J ($g/m^2 \cdot h$)	α	Ref.
PDMS	40	11.9	25	14	7.1	(4)
Symmetric PDMS on PP membrane	25	5	30	136	9.78	(5)
Zeolite-filled PDMS/PS composite membrane	–	4.8	60	231.3	7.52	(6)
PDMS-PS IPN supported membrane	15	10	60	160	5.5	(7)
PDMS/PEI/PPP composite membrane	40	5	40	270	3.7	(8)
1060 Sulzer PDMS commercial membrane	–	13	40	800	2.1	(9)
PDMS-Zeolite Pervap 1070 membrane	30.5	4.5	80	600	11.4	(10)
PDMS/PA composite membrane	1	2.5	30	620	7.9	(11)
PDMS/PVDF/PP composite membrane	10	2	60	600	9.2	This
		5	60	800	7.8	study

Effect of Feed Flow Rate

The effect of the Reynolds number on the flux and ethanol selectivity at different feed temperatures for a 2% ethanol solution under a fixed permeate-side pressure of 1 mmHg is shown in Fig. 4. The total flux and ethanol selectivity increased slightly versus the Reynolds numbers of 500 to 2500 at all feed temperatures. The total flux and ethanol selectivity increased by about 5% and 3%, respectively, at feed temperature of 60°C. The feed volumetric flow rate thus had minimal impact on the ethanol enrichment in the permeate.

Effect of Feed Concentration

The permselective properties of pervaporation membranes are determined by sorption and diffusion of the permeating components in the membrane. Because both sorption and diffusion phenomena depend on the composition of the liquid mixture, membrane permeation characteristics are usually strongly influenced by the feed composition. The influence of the ethanol content in the feed mixture on the pervaporation performance is shown in Fig. 5.

The total and ethanol flux increased with increasing in the feed ethanol concentration from 2–70%wt., as shown in Figs. 5a and 5b, respectively. For more concentrated mixtures, the ethanol and total flux increased very sharply. The results obtained are in agreement with the general tendency, that is, when the membrane is in contact with concentrated feed solutions, the swelling of the membrane is higher. Ethanol and water molecules can diffuse faster through the membrane, and thus, higher permeation fluxes can be observed. The increase of permeation flux with feed ethanol concentration that interacts strongly with the membrane might be explained by using the dependence of thermodynamic and kinetic parameters on concentration. Slater et al. (5), Li and Wang (6), Shi et al. (11) and Garcia et al. (38) determined that the permeation flux in PDMS membranes increased with ethanol concentration in the same way as reported in this work.

The dependence of ethanol selectivity on the feed concentration is depicted in Fig. 5c. It can be seen that the ethanol selectivity decreased as the ethanol content of the feed mixture increased. As discussed before, a change in the feed composition affected the sorption phenomena at the liquid/membrane interface. The mixture components activity can be varied more or less by the change in composition depending on the chemical nature of the mixture. In general, the higher the content of the component that interacts strongly with the polymer, the better the swelling is,

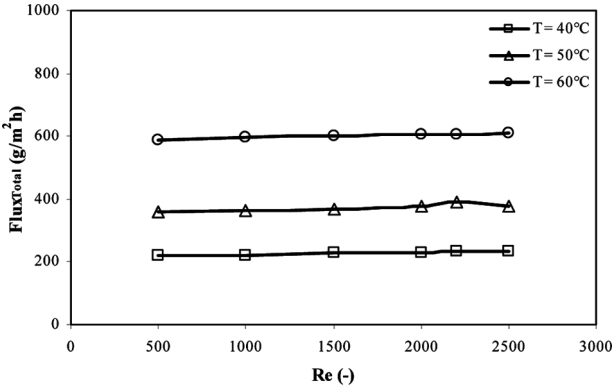

(a)

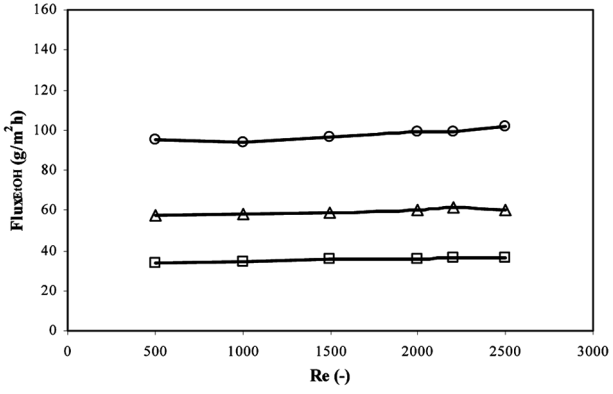

(b)

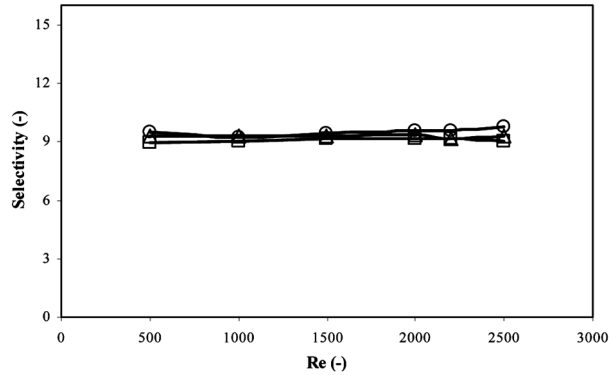

(c)

Figure 4. Effect of Reynolds number on (a) total flux, (b) ethanol flux, and (c) ethanol selectivity at different feed temperatures ($C_o = 2\%$wt., $P_P = 1$ mmHg).

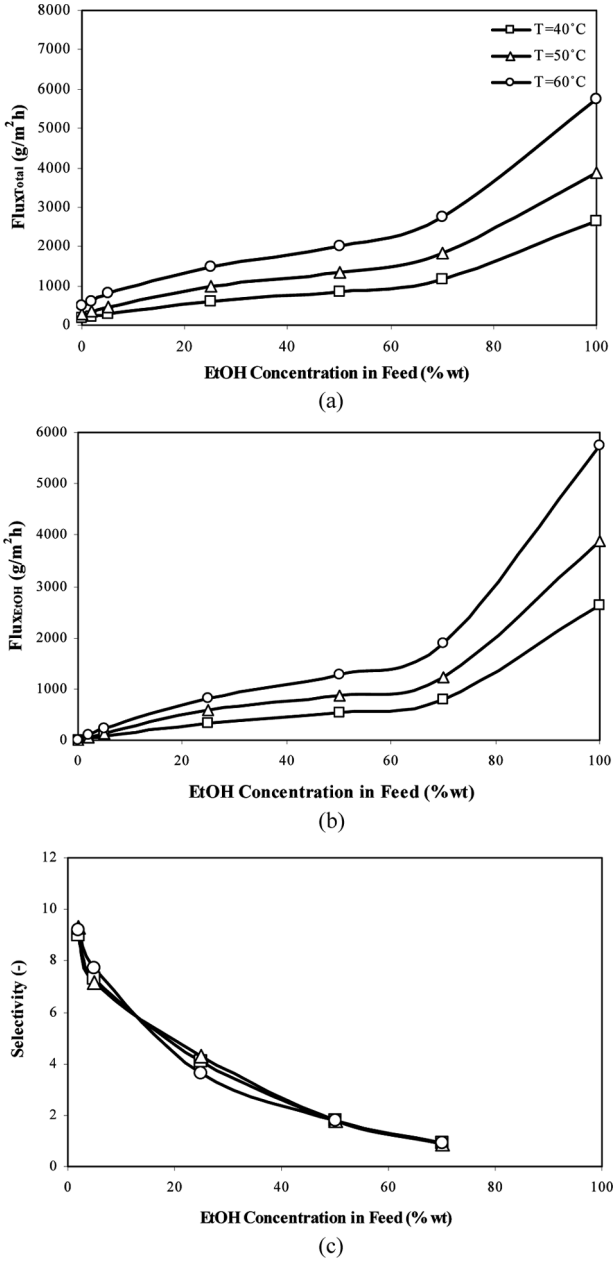

Figure 5. Effect of feed concentration on (a) total flux, (b) ethanol flux, and (c) ethanol selectivity at different feed temperatures ($Re = 1000$, $P_P = 1$ mmHg).

and thus, the amount of lower affinity molecules that diffuse through the membrane is higher. On the other hand, when the content of the preferential component in the mixture is lower, the swelling is less extended and consequently, the selectivity of the process is higher.

Effect of Permeate-Side Pressure

Another important parameter that affects the performance of the pervaporation process is the permeate-side pressure. The dependence of the flux and ethanol selectivity on the permeate-side pressure for a 2% ethanol feed solution at different feed temperatures is shown in Fig. 6. The total flux curves showed a non-linear decrease at all temperatures as the permeate-side pressure was increased. Due to reduced driving force, the permeation rate dropped and reached to zero as the permeate-side pressure approached permeant vapor pressure. According to the pseudophase-change solution-diffusions model (39,40), the permeate-side pressure also affects the pressure profile as well as the liquid transfer depth within the membrane, lower pressure inducing a higher pressure gradient within the membrane, and decreasing the liquid transfer depth. As the permeate-side pressure increases, the liquid transfer depth penetrates into the vapor transfer space and mass transfer becomes dominated by the slower liquid transfer, decreasing the total permeation rate. These results are different from those of some other authors who reported that downstream pressure does not affect the flux and the selectivity for ethanol/benzene and ethanol/cyclohexane systems (41), but agree well with the results of Li and Wang (6). They used Zeolite-filled polydimethylsiloxane/polysulfone composite membranes to separate ethanol from dilute ethanol/water mixtures and observed that the permeation flux decreases with increasing downstream pressure while the ethanol selectivity rises.

The effect of the permeate-side pressure on the ethanol selectivity at various feed temperatures is presented in Fig. 6c. It was shown that the feed temperature had little effect on the selectivity while the permeate-side pressure was held below 20 mmHg but had a significant effect at the permeate-side pressures above 20 mmHg, at which the selectivity increased as much as four-fold. This suggests that more ethanol can pass through the membrane when the liquid transfer depth increases relative to the vapor transfer depth within the membrane. On the other hand, ethanol may pass more readily than water through the wet space inside the membrane. The selectivity may therefore be determined by the liquid transfer depth and will be greater when the permeate-side pressure approaches the solution vapor pressure.

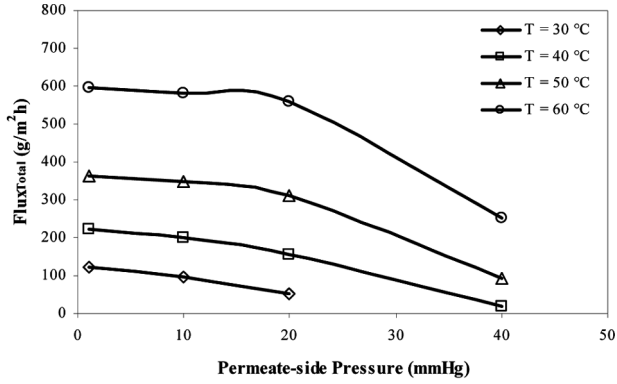

(a)

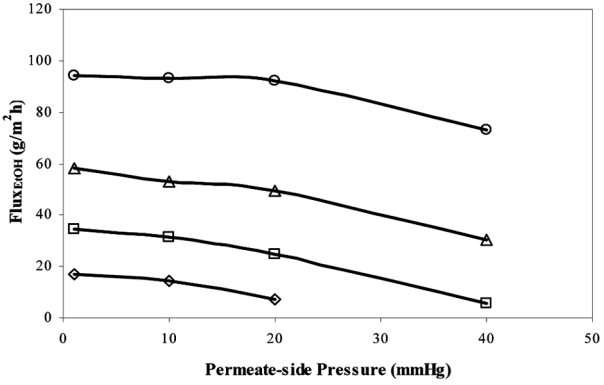

(b)

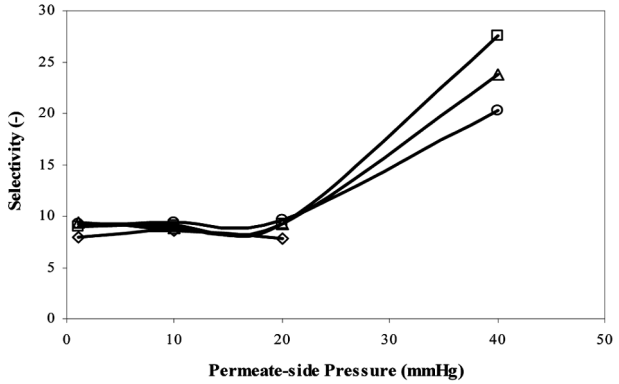

(c)

Figure 6. Effect of permeate-side pressure on (a) total flux, (b) ethanol flux, and (c) ethanol selectivity at different feed temperatures ($C_o = 2\%$wt., $Re = 1000$).

Depending on the relative volatility of the permeating components, selectivity may rise or drop with increase in the permeate-side pressure (42). If the more rapidly permeating species is also the more volatile, the selectivity increases as the permeate-side pressure is raised. In the opposite case, the less volatile component is more rapidly permeating species, the selectivity decreases as the permeate-side pressure increases. Increasing in selectivity of ethanol can be explained according to this law. Ethanol is more volatile than water, and showed higher permeability through the PDMS membrane. Therefore, ethanol selectivity increased as the permeate-side pressure was raised. A similar result was reported using symmetric PDMS on the PP membrane for the separation of ethanol from a 5%wt. ethanol/water mixture (5) and using a PDMS composite membrane for orange juice aroma compounds recovery (34).

Effect of Feed Temperature

In pervaporation, the feed temperature is an important parameter since this parameter affected the feed/membrane characteristics and the driving force of process. The influence of feed temperatures on the permeation flux for pervaporation of 2% ethanol solutions is presented in Figs. 6a and 6b. The total flux increased significantly with increasing feed temperature, especially at the lower permeate-side pressures. This agrees with the common results obtained by other researchers. They have also observed that permeation flux enhances with an increase in the feed temperature (5,6,9,11).

It is known that the diffusivity and viscosity of components in feed and permeability of these compounds into the membrane are affected by the temperature variation in the feed. According to the free volume theory in polymeric membrane, the permeating molecules diffuse through the free volumes of the membrane. The free volume in a polymeric membrane can be made from segmental motions of the polymer chain in the amorphous regions. When the feed temperature goes to a higher degree, a segmental motion into the membrane polymer chain will be increased. As a result, the free volume in the membrane increases, thus the diffusion rate of the individual permeating molecules increases, leading to a high permeation flux as the temperature increases. In addition, as the equilibrium vapor pressure of the permeating molecules varies with temperature, the feed temperature influences the driving force of the process. Increasing in equilibrium vapor pressure of the pure component due to the increase of feed temperature, results in high permeation flux.

Figure 7 shows that the ethanol selectivity did not change significantly at different feed temperatures while the permeate-side pressure

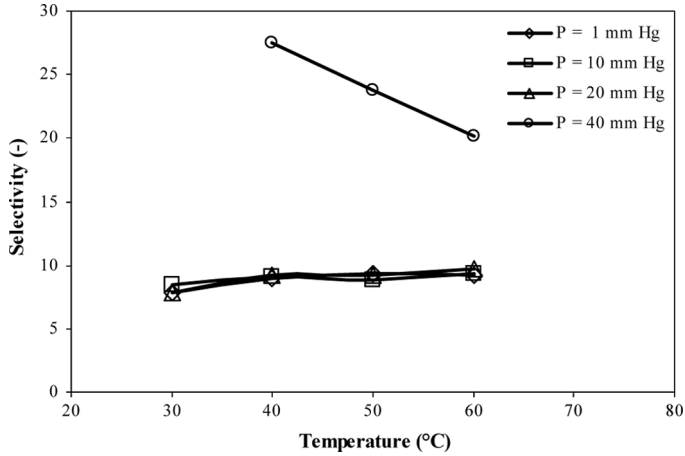

Figure 7. Effect of feed temperature on ethanol selectivity at different permeate-side pressures ($C_o = 2\%$wt., $Re = 1000$).

was held below 20 mmHg. But when the permeate-side pressure was held at 40 mmHg, the selectivity decreased significantly as the feed temperature increased. The solution vapor pressure at a feed temperature of 40°C is very close to this pressure, thus filling the membrane with liquid and increasing the selectivity. At feed temperatures of 50 and 60°C and a permeate-side pressure of 40 mmHg, the solution vapor pressure increased and the liquid transfer depth within the membrane decreased which partially explains why the selectivity decreases beyond 40°C at the permeate-side pressure of 40 mmHg.

Consequently, in pervaporative ethanol separation from aqueous solutions with PDMS membranes, the feed temperature should be as high as possible to improve the performance; however, the maximum feed temperature that can be applied is limited by the nature of the feed and the membrane.

Mass Transport Resistances

The resistance-in-series model was used to calculate the mass transfer resistances in the pervaporation process of ethanol/water mixtures with the composite PDMS membrane. In the following, a parametric study of the purposed model is performed.

All the resistances were positive except for the liquid boundary resistances of water, which were negative, indicating that the transport of water was in the opposite direction to ethanol. On the other hand, the

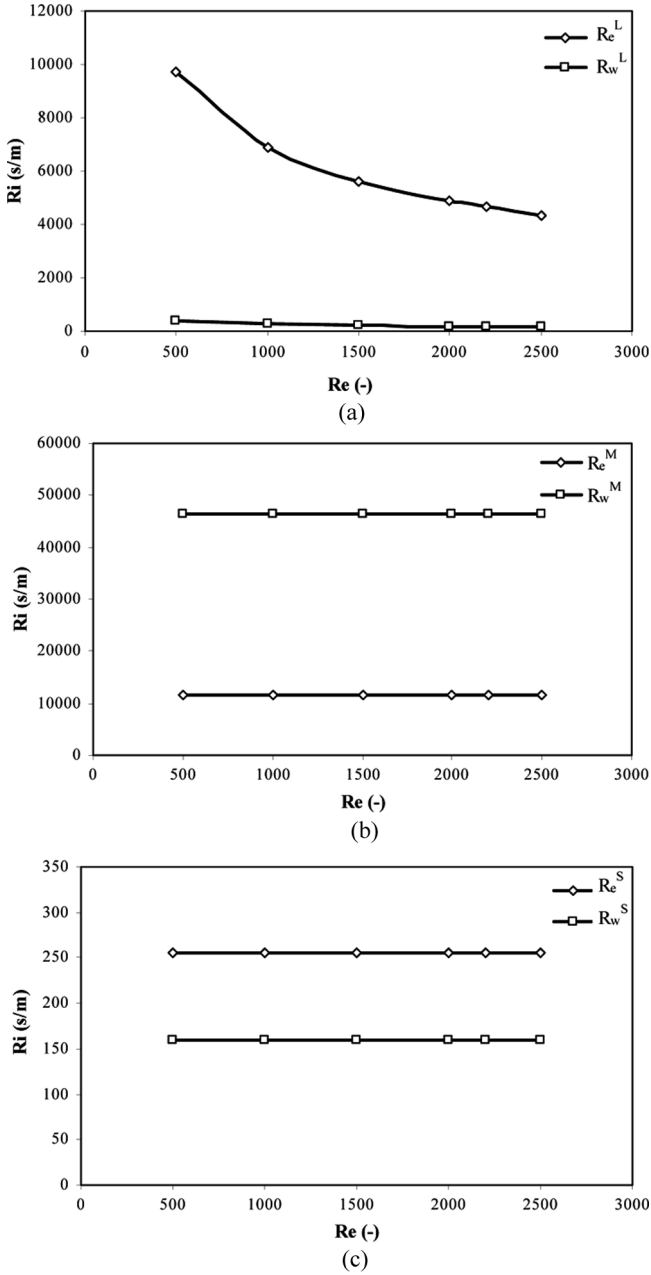

Figure 8. Effect of Reynolds number on transport resistances ($C_o = 2\%$wt., $T = 40°C$, $P_P = 1$ mmHg, R_w^L is a negative value and that the plots show the absolute values).

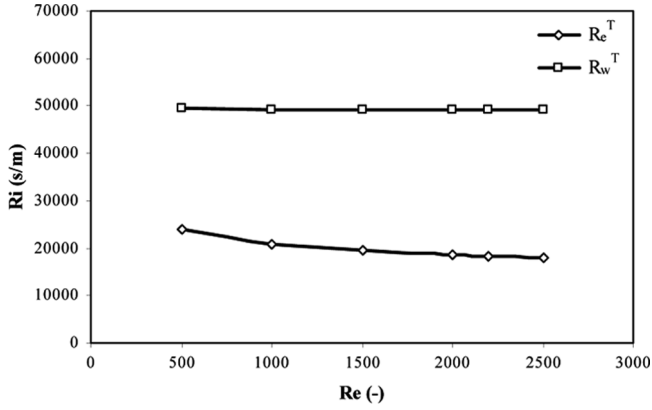

(d)

Figure 8. Continued.

diffusive transport of water in the boundary layer was from the liquid/membrane interface to the bulk phase. The absolute value of R_w^L is reported in Figs. 8–10.

For both components, the membrane active layer resistances were the main resistance to transport and the liquid boundary and the support layer resistances were low and negligible, respectively. This agrees with the common results obtained by other researchers. For pervaporation dehydration of ethanol/water mixtures with chitosan/hydroxyethylcellulose (CS/HEC) composite membranes, both the liquid boundary and the support layer resistances were also found to be negligible (13). However, for very dilute systems such as pervaporation separation of ethylbutanoate solution by polyether block amide (PEBA) membranes (43), analysis of the resistances showed that the transport resistance in the liquid boundary layer for ethylbutanoate was highest, and therefore, was the controlling resistances for the system.

Effect of Feed Flow Rate

The influence of the feed flow rate, which is corresponds to the Reynolds number, on the mass transport resistances for pervaporation of a 2%wt. ethanol solution at 40°C and the permeate-side pressure of 1 mmHg is shown in Fig. 8. The liquid boundary layer resistance to the transport of ethanol was much higher than that of water, as shown in Fig. 8a. This indicates that ethanol transport was more difficult due to its low concentration and diffusion in the liquid boundary layer. The ethanol and water

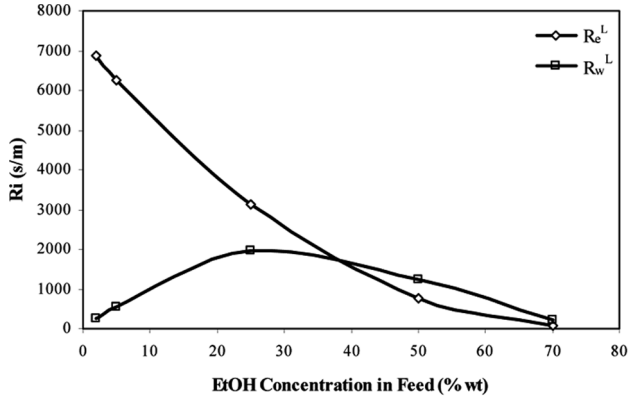

(a)

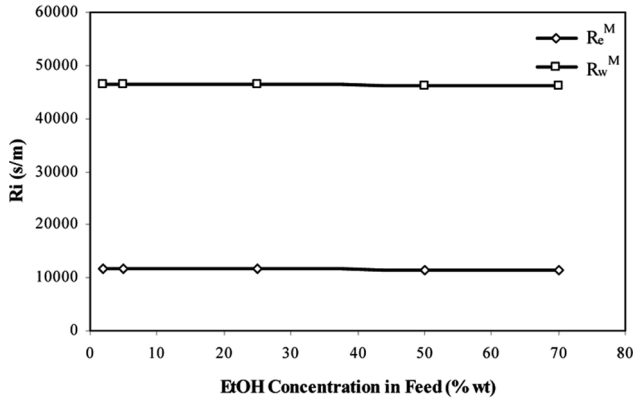

(b)

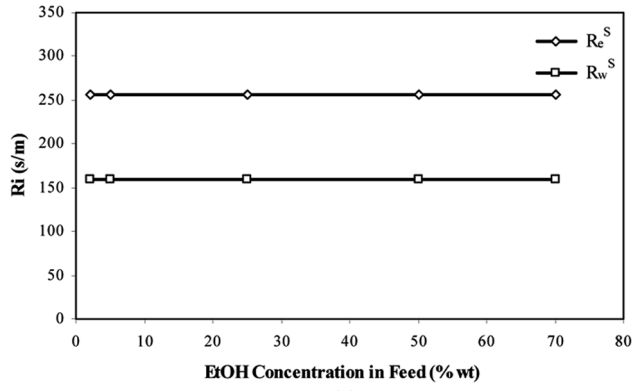

(c)

Figure 9. Effect of feed concentration on transport resistances ($T = 40°C$, $Re = 1000$, $P_P = 1$ mmHg, R_w^L is a negative value and that the plots show the absolute values).

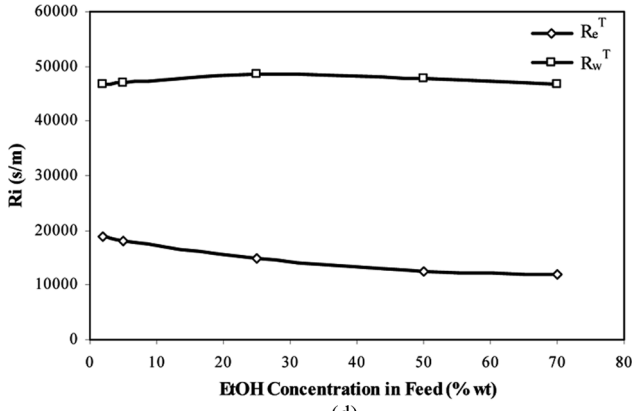

(d)

Figure 9. Continued.

liquid boundary resistances decreased with increasing Reynolds number, but decreasing of R_e^L is more significant. When the Reynolds number was increased, the mass transfer coefficient of ethanol in water enhanced due to increasing of mixing and relative turbulency in the liquid boundary layer, consequently the mass transport coefficient, k_L, increased. Therefore, a reduction in R_e^L and absolute R_w^L was observed due to an increase of k_L.

For the resistances in the membrane active layer, it was found that R_w^M was higher than R_e^M as shown in Fig. 8b. This indicates that ethanol could be transported more easily than water due to the affinity of ethanol molecules to the hydrophobic PDMS membrane; however, the ethanol diffusion coefficient in the membrane ($2.16 \times 10^{-10}\,m^2/s$) is lower than that of water ($8.67 \times 10^{-9}\,m^2/s$). Variation in the feed flow rate had no significant effect on the membrane active layer and the porous support layer resistances. It can be seen from Fig. 8c that R_e^S was higher than R_w^S. The reason is that the water molecule is smaller than the ethanol molecule, so the transport of water in the porous support layer is easier.

Effect of Feed Concentration

Variation of the mass transport resistances with increasing of ethanol concentration in the feed solution are presented in Fig. 9. It can be seen that R_e^L was lower than R_w^L for higher ethanol content, and R_e^L decreased as ethanol concentration in the liquid mixtures increased but R_w^L showed a maximum. According to Eq. (10), a decrease of R_i^L can be related to the

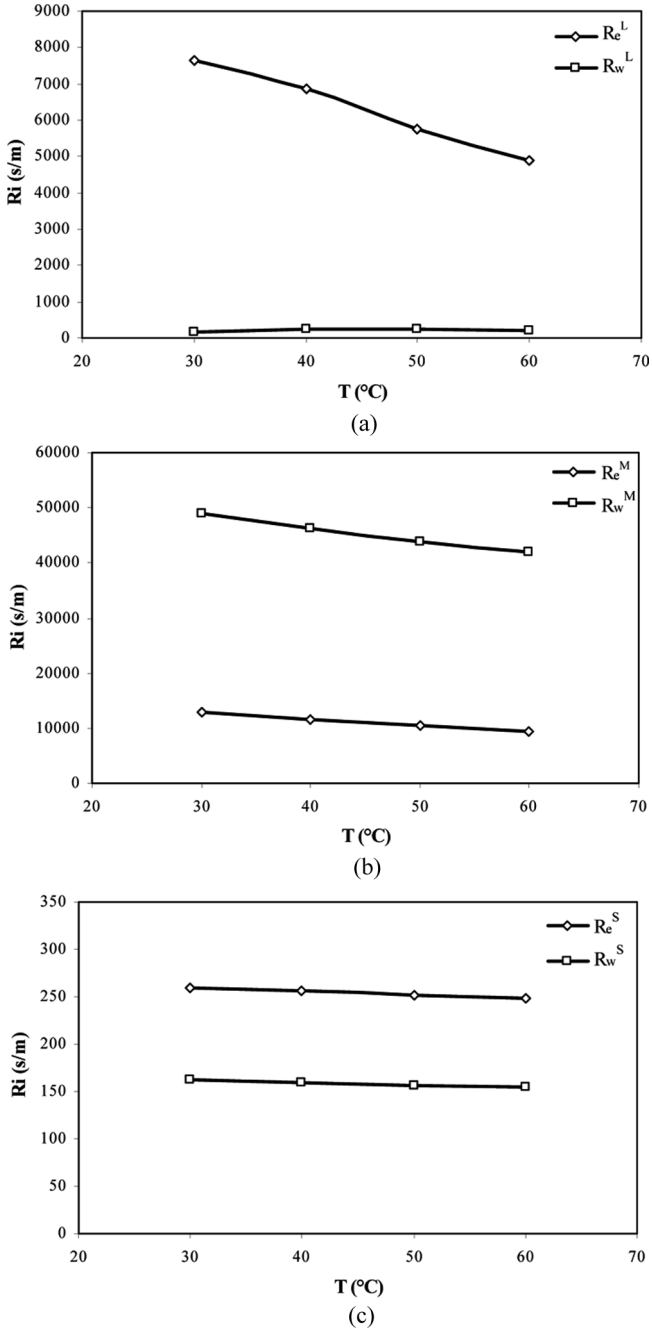

Figure 10. Effect of feed temperature on transport resistances ($C_o = 2\%$wt., $Re = 1000$, $P_P = 1$ mmHg, R_w^L is a negative value and that the plots show the absolute values).

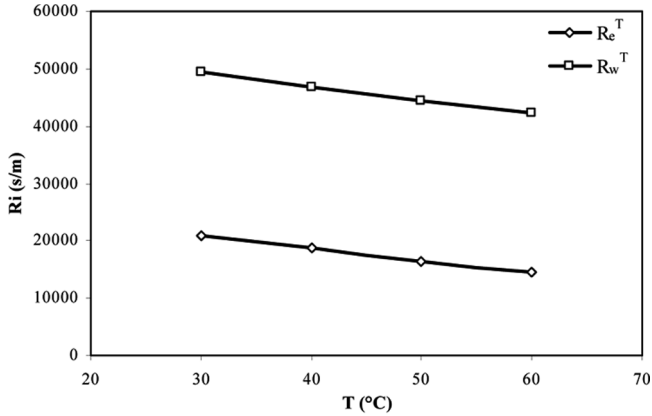

(d)

Figure 10. Continued.

decrease of the enrichment factor and permeate velocity as well as to the increase of molar density and mass transfer coefficient in the liquid boundary layer. A reduction of the ethanol boundary layer resistance with increasing in its concentration in the feed solution was attributed to a decrease of the enrichment factor and to an increase of C_L. For water, β_w and C_L rise as ethanol concentration in the feed increases, thus an enhancement of R_w^L at low ethanol concentration and a decrease of it at high ethanol concentration can be related to increase of β_w and C_L, respectively. This leads to the conclusion that the influence of β_w on R_w^L is more than C_L at low ethanol concentration.

The membrane active layer resistances decreased slightly with ethanol content in the feed solution. The reason is that an increase of sorption in the membrane caused an increase of ethanol concentration in the membrane active layer, resulting in slight membrane swelling. Therefore, the membrane enrichment factor increased and leads to the reduction of R_i^M. As can be observed from Fig. 9c, the support layer resistances did not vary with ethanol concentration.

Effect of Feed Temperature

The dependence of resistances on the feed temperature is depicted in Fig. 10. All mass transport resistances decreased as the feed temperature varied from 30 to 60°C. An increase of feed temperature led to enhance the diffusion coefficient in the boundary layer and the membrane active layer as well as higher ethanol and water sorption in the membrane, thus

R_i^L and R_i^M decreased. Also, according to Eq. (12), there is an inverse relation between R_i^S and $T^{0.5}$, so the support layer resistances decreased at high feed temperatures.

CONCLUSIONS

An experimental study was conducted on the sorption and pervaporation process for the separation of ethanol from its aqueous solutions. It can be concluded that pervaporation is an attractive technique to separate ethanol from dilute ethanol/water mixture. The results showed that the total flux and ethanol selectivity did not change significantly versus the Reynolds number at different feed temperatures, and their variations versus the Reynolds numbers of 500 to 2500 were about 5% and 3%, respectively. As ethanol concentration in the feed solution increased, the total and ethanol flux enhanced but the ethanol selectivity dropped from 9.3 to 0.9 as the feed ethanol concentration varied from 2 to 70%wt. The total flux markedly increased as the feed temperature increased. The ethanol selectivity did not increase significantly at the permeate-side pressures below 20 mmHg, but increased at pressures above 20 mmHg. Both the total and ethanol flux decreased nonlinearly as the permeate-side pressure increased.

A resistances-in-series model was used for the analysis of mass transport across a composite PDMS membrane. As shown in this work, mass transport was controlled by the resistance of components in the membrane active layer and transport resistances in the liquid boundary layer and in the support layer were low and negligible, respectively. Except R_e^M, other transport resistances for ethanol were relatively high compared to water resistances. An increase in the feed flow rate led to constant R_i^M and R_i^S, while R_i^L decreased. This implies that the system should be operated at high feed flow rates or Reynolds numbers. Variation in the feed ethanol concentration resulted in a significant effect on the boundary layer resistances and a minor effect on the membrane active layer resistances. Also, all mass transport resistances were found to decrease with temperature.

The results are expected to enhance the fundamental understanding and contribute to further development of the efficient pervaporation systems.

ACKNOWLEDGEMENTS

The authors would like to thank GKSS Forschungszentrum (Geesthacht, Germany) for supplying the PDMS membranes.

LIST OF SYMBOLS

Nomenclature

a_i	activity of component *i*
C_o	feed concentration (%wt.)
C_i	molar concentration of component i (kmol/m^3)
C_L	molar density of liquid feed (kmol/m^3)
d_p	pore diameter (m)
D_i	diffusion coefficient of component *i* (m^2/s)
$D_{o,i}$	diffusion coefficient of component *i* the membrane at infinite dilution (m^2/s)
E_i	energy required to overcome attractive forces from neighboring molecules (cal/mol)
J	total molar flux (kmol/m$^2 \cdot$ s)
J_i	partial molar flux of component *i* (kmol/m$^2 \cdot$ s)
k_L	mass transfer coefficient in liquid boundary layer (m/s)
$K_{I,i}$	solvent free volume parameter (cm^3/g $\cdot$ K)
$K_{II,i}$	solvent free volume parameter (K)
$K_{I,p}$	polymer free volume parameter (cm^3/g $\cdot$ K)
$K_{II,p}$	polymer free volume parameter (K)
M_i	molecular weight of component *i* (kg/kmol)
P_P	permeate pressure (mmHg)
R	gas constant
Re	Reynolds number
R_i^L	liquid boundary layer resistance of component *i* (s/m)
R_i^M	membrane active layer resistance of component *i* (s/m)
R_i^S	support layer resistance of component *i* (s/m)
R_i^T	total resistance of component *i* (s/m)
S	area of the membrane (m^2)
T	temperature (K)
$T_{g,i}$	solvent glass transition temperature (K)
$T_{g,p}$	polymer glass transition temperature (K)
T_s	temperature in porous support (K)
$\widehat{V}^{FH}$	total hole free volume (cm^3/g)
$\widehat{V}_i^*$	specific critical hole free volume of solvent required for jump (cm^3/g)
v_p	permeate molar average velocity (m/s)
$\widehat{V}_p^*$	specific critical hole free volume of polymer required for jump (cm^3/g)
W	weight of collected permeate (g)

w_i weight fraction of component *i*
w_p weight fraction of polymer
x_i mole fraction of component *i*

Greek Letters

α_{ij} separation factor
$\alpha_{i,j}^S$ sorption selectivity
β_i enrichment factor
β_i^M enhancement factor
χ porous support porosity
δ_M membrane thickness (m)
δ_S porous support thickness (m)
ε porous support tortuosity
γ overlap factor which accounts for shared free volume
ρ_i density of component i (kg/m^3)
ρ_m density of liquid mixture (kg/m^3)
τ time of pervaporation experiment (h)
ξ_{ip} ratio of critical molar volume of solvent jumping unit to that of polymer jumping unit

Subscripts

1 liquid boundary/membrane active layer interface
2 membrane active layer/support layer interface
e ethanol
i component index
j component index
w water

Superscripts

F Feed
L Liquid
M Membrane
P Permeate
S Support

REFERENCES

1. Kim, H.J.; Nah, S.S.; Min, B.R. (2002) A new technique for preparation of PDMS pervaporation membrane for VOCs removal. *Adv. Environ. Res.*, *6*: 255.
2. Feng, X.; Huang, R.Y.M. (1997) Liquid separation by membrane pervaporation: A review. *Ind. Eng. Chem. Res.*, *36*: 1048.

3. Goncalves, M.D.C.; Marques, G.D.S.S.; Galembeck, F. (1983) Pervaporation and dialysis of water–ethanol solutions using silicone rubber membranes. *Sep. Sci. Technol.*, *18* (10): 893.
4. Changliu, Z.; Moe, L.; We, X. (1987) Separation of ethanol–water mixtures by pervaporation-membrane separation process. *Desalination*, *62*: 299.
5. Slater, C.S.; Hickey, P.J.; Juricic, F.P. (1990) Pervaporation of aqueous ethanol mixtures through poly(dimethy1siloxane) membranes. *Sep. Sci. Technol.*, *25* (9): 1063.
6. Li, X.; Wang, Sh. (1996) Some characteristics of pervaporation for dilute ethanol-water mixtures by alcohol-permselective composite membrane. *Sep. Sci. Technol.*, *31* (20): 2867.
7. Liang, L.; Ruckenstein, E. (1996) Pervaporation of ethanol–water mixtures through polydimethylsiloxane–polystyrene interpenetrating polymer network supported membranes. *J. Membr. Sci.*, *114* (2): 227.
8. Galindo, M.O.; Clar, A.I.; Miranda, I.A.; Greus, A.R. (2001) Characterization of poly(dimethylsiloxane)–poly(methyl hydrogen siloxane) composite membrane for organic water pervaporation separation. *J. Appl. Poly. Sci.*, *81* (3): 546.
9. Molina, J.M.; Vatai, G.; Bekassy-Molnar, E. (2002) Comparison of pervaporation of different alcohols from water on CMG-OM-010 and 1060-SULZER membrane. *Desalination*, *149*: 89.
10. Lipnizki, F.; Hausmanns, S. (2004) Hydrophobic pervaporation of binary and ternary solutions: evaluation of fluxes, selectivities, and coupling effects. *Sep. Sci. Technol.*, *39* (10): 2235.
11. Shi, E.; Huang, W.; Xiao, Z.; Li, D.; Tang, M. (2007) Influence of binding interface between active and support layers in composite PDMS membranes on permeation performance. *J. Appl. Poly. Sci.*, *104* (4): 2468.
12. Liu, M.G.; Dickson, J.M.; Cote, P. (1996) Simulation of a pervaporation system on the industrial scale for water treatment. Part I. Extended resistance-in-series model. *J. Membr. Sci.*, *111* (2): 227.
13. Jiraratananon, R.; Chanachai, A.; Huang, R.Y.M. (2002) Pervaporation dehydration of ethanol–water mixtures with chitosan/hydroxyethylcellulose (CS/HEC) composite membranes. II. Analysis of mass transport. *J. Membr. Sci.*, *199* (1–2): 211.
14. Henis, J.M.S.; Tripodi, M.K. (1981) Composite hollow fiber membrane for gas separation: the resistance model approach. *J. Membr. Sci.*, *8* (2): 238.
15. Gudematsch, W.; Menzel, T.; Strathmann, H. (1991) Influence of composite membrane structure on pervaporation. *J. Membr. Sci.*, *61* (1): 19.
16. Ji, W.; Sikdar, S.K.; Hwang, S.-T. (1994) Modeling of multicomponent pervaporation from removal of volatile organic compounds from water. *J. Membr. Sci.*, *93* (1): 1.
17. Raghunath, B.; Hwang, S.-T. (1992) Effect of boundary layer mass transfer resistance in pervaporation of dilute organics. *J. Membr. Sci.*, *65* (1–2): 147.
18. Pinho, M.N.De.; Rautenbech, R.; Herion, C. (1990) Mass transfer in radiation grafted pervaporation membranes. *J. Membr. Sci.*, *54* (1–2): 131.

19. Sferrazza, R.A.; Escobosa, R.; Gooding, C.H. (1988) Estimation of parameters in a sorption–diffusion model of pervaporation. *J. Membr. Sci.*, *35* (2): 125.
20. Choi, H.S.; Hino, T.; Shibata, M.; Negishi, Y.; Ohya, H. (1992) The characteristics of a PAA–PSf composite membranes for a separation of water–ethanol mixtures through pervaporation. *J. Membr. Sci.*, *72* (3): 259.
21. Koops, G.H.; Nolten, J.A.M.; Mulder, M.H.V.; Smolders, C.A. (1993) Poly(vinyl chloride)/polyacrylonitrile composite membranes for the dehydration of acetic. *J. Membr. Sci.*, *81* (1–2): 57.
22. Ohya, H.; Shibata, M.; Negishi, Y.; Guo, Q.H.; Choi, H.S. (1994) The effect of molecular weight cut-off of PAN ultrafiltration support layer on separation of water–ethanol mixtures through pervaporation with PAA–PAN composite membrane. *J. Membr. Sci.*, *90* (1–2): 91.
23. Brian, P.L.T. (1996) Mass Transport in Reverse Osmosis, In: *Desalination by Reverse Osmosis*; U. Merten (Ed.), M.I.T. Press: Cambridge, MA.
24. Cussler, E.L. (1989) *Diffusion*; Cambridge University Press: New York.
25. Schofield, R.W.; Fane, A.G.; Fell, C.J.D. (1990) Gas and vapor transport through microporous membranes. I. Knudsen–Poiseuille transition. *J. Membr. Sci.*, *53* (1–2): 159.
26. Fredenslund, A.; Gmehling, J.; Rasmussen, P. (1977) *Vapor-Liquid Equilibria Using UNIFAC*; Elsevier: Amsterdam.
27. Oishi, T.; Prausnitz, J.M. (1978) Estimation of solvent activities in polymer solutions using a group-contribution method. *Ind. Eng. Chem. Proc. Des. Dev.*, *17* (3): 333.
28. Cohen, M.H.; Turnbull, D. (1959) Molecular transport in liquids and gases. *J. Chem. Phys.*, *31* (5): 1164.
29. Vrentas, J.S.; Duda, J.L. (1977) Diffusion in polymer–solvent systems. II. A predictive theory for the dependence of diffusion coefficients on temperature, concentration and molecular weight. *J. Polym. Sci. Pol. Phys.*, *15*: 417.
30. Vrentas, J.S.; Duda, J.L.; Ling, H.C. (1984) Self diffusion in polymer–solvent–solvent systems. *J. Polym. Sci. Pol. Phys.*, *22*: 459.
31. Zielinski, J.M.; Duda, J.L. (1992) Predicting polymer/solvent diffusion coefficients using free-volume theory. *AIChE J.*, *38* (3): 405.
32. Hong, S.U. (1995) Prediction of polymer solvent diffusion behavior using free-volume theory. *Ind. Eng. Chem. Res.*, *34* (7): 2536.
33. Aroujalian, A.; Belkacemi, K.; Davids, J.; Pouliot, Y.; Turcotte, G. (2003) Effect of protein on flux and selectivity in pervaporation of ethanol from a dilute solution. *Sep. Sci. Technol.*, *38* (12–13): 3239.
34. Aroujalian, A.; Raisi, A. (2007) Recovery of volatile aroma components from orange juice by pervaporation. *J. Membr. Sci.*, *303* (1–2): 154.
35. Poling, B.E.; Prausnitz, J.M.; O'Connell, J.P. (2001) *The Properties of Gases and Liquids,* 5th Ed.; McGraw Hill: New York.
36. Perry, R.H.; Green, D. (1997) *Perry's Chemical Engineers' Handbook,* 6th Ed.; McGraw-Hill: New York.
37. Kennard, E.H.. (1938) *Kinetic Theory of Gases*; McGraw-Hill: New York.

38. Garcia, M.E.F.; Habert, A.C.; Pires, L.A.; Nobrega, R. (1991) The Use of PDMS and EVA Membranes to Remove Ethanol during Fermentation, In *Proceedings of the Fifth International Pervaporation Process in the Chemical Industry*; R. Bakish (Ed.), Bakish Material Corp.: Englewood, NJ.
39. Shieh, J.; Huang, R.Y.M. (1998) A pseudophase-change solution-diffusion mode1 for pervaporation I. Single component permeation. *Sep. Sci. Technol.*, *33* (6): 767.
40. Shieh, J.; Huang, R.Y.M. (1998) A pseudophase-change solution-diffusion mode1 for pervaporation II. Binary mixture permeation. *Sep. Sci. Technol.*, *33* (7): 993.
41. Li, X.; Wang, S. (1994) A Mass Transfer Model for Pervaporation of Ethanol-Water Mixture by Zeolite-Filled PDMS Membrane, In: *Proceeding of International Symposium on Membrane and Membrane Processes*: Hongzhou, People's Republic of China.
42. Noble, R.D.; Stern, S.A. (1995) *Membrane Separations Technology: Principles and Applications*; Elsevier: Amsterdam.
43. Jiraratananon, R.; Sampranpiboon, P.; Uttapap, D.; Huang, R.Y.M. (2002) Pervaporation separation and mass transport of ethylbutanoate solution by polyether block amid (PEBA) membranes. *J. Membr. Sci.*, *210* (2): 389.